

Free Energy Grids: A Practical Qualitative Application of Free Energy Perturbation to Ligand Design Using the OWFEG Method

David A. Pearlman*

Vertex Pharmaceuticals Incorporated, 130 Waverly Street, Cambridge, Massachusetts 02139-4242

Received March 22, 1999

Traditional window-based free energy calculations can precisely determine the free energy corresponding to a molecular change of interest. However, calculations performed in this fashion are typically slow and resource-intensive, which renders them less than ideal for drug design. To circumvent this drawback, a new approximate free energy method, OWFEG, has been developed and tested. OWFEG replaces the exact free energy calculation for a single change with a set of approximate calculations for a grid of possible changes surrounding a molecule. One of the key features of OWFEG is that a floating independent reference frame (FIRF) is used, so that each grid point moves with the region of the molecule to which it is closest. In this way, this approach has been made applicable to flexible molecules. OWFEG is applied to two model systems and then to the FKBP-12·FK506 protein–ligand complex. On the basis of the results of these tests, this approximate method shows promise as a predictive tool for drug design.

Introduction

The earliest applications of free energy perturbation calculations to nontrivial systems were reported in the early 1980s.^{1–3} These calculations—which for the first time offered the possibility of using molecular dynamics to precisely determine the free energy associated with a molecular change—generated substantial excitement and spurred substantial work in the field. The ensuing decade and a half have witnessed considerable efforts devoted toward characterizing and refining free energy methods.⁴ It has been demonstrated that the methods can reliably be applied to select systems of interest, provided they are carefully carried out and analyzed.^{5,6}

A key to reliable application of free energy methods is ensuring that the simulations are run to convergence. Free energy simulations require the evaluation of averages from an ensemble of configurations that are generated using either molecular dynamics⁷ or a Monte Carlo⁸ random walk. It has repeatedly been shown that convergence of the requisite ensembles requires they be determined from very large numbers of configurations.^{9–17} For example, in the case of molecular dynamics, hundreds of thousands of configurations are typically required. Generation and evaluation of each configuration is costly, and so these simulations are typically expensive in terms of computer resources and frequently slow in terms of real time to carry out.

This presents a problem when one attempts to apply free energy simulation toward the goal of drug design. In the initial stages of drug design, one has typically identified a ligand lead and wishes to improve its binding efficacy. The question at this stage is not “what will be the effects of a particular change?” but rather more generally “what changes can be made to improve the binding constant?” Unfortunately, standard high-precision free energy simulations are only practicable for answering the first question.

It is this limitation of high-precision free energy calculations that led to the search for alternate, approximate, free energy methods that *could* be useful in answering more general questions of direction in drug design. Here we describe and characterize such a method, OWFEG (one-window free energy grid), which is based on an approximate application of the free energy perturbation method. Using OWFEG, the free energy for introducing a probe group at a matrix of grid points surround a ligand is estimated from a single one-window free energy perturbation calculation. Then, using a contour plot derived from the results, one can determine, qualitatively, where the probe group can be added to the ligand to best achieve the desired changes in free energy properties. Flexibility of the ligand is accommodated by use of an independent reference frame for each grid point. A comparison of OWFEG grids with the actual calculated free energies for changes at each position on the ligand demonstrates the feasibility of this approach.

Background

Free energy calculations are based on fundamental equations that can be derived from classical statistical mechanics.⁴ Two different fundamental equations lead to two different free energy methods. The first, free energy perturbation (FEP), is based on the equation:

$$\Delta G = G_B - G_A = -RT \ln \langle e^{-(V_B - V_A)/RT} \rangle_A \quad (1)$$

which relates the free energy between two molecular states “A” and “B” to the ensemble average of a quantity that depends on the difference in the potential energies for those states. G_B and G_A are the respective free energies of states B and A. “ $\langle \rangle_A$ ” refs to the average of the quantity within the brackets, evaluated from an ensemble representative of state A. V_B and V_A are the potential energies of the respective states, evaluated for the same configuration of the system. R is the gas constant, and T is the temperature.

Note that in order to properly evaluate the average, it is crucial that the ensemble includes not only configurations that are favorable for state "A" but also configurations that are favorable for state "B". But the ensemble is generated using the potential function for state A. Therefore, if the endpoints "A" and "B" are too dissimilar, favorable "B" configurations within the ensemble will be underrepresented, and the free energy difference will fail to properly converge. To circumvent this problem, a λ parameter is introduced into the analytical potential function such that $V(\lambda=0, \mathbf{x})$ represents state A, $V(\lambda=1, \mathbf{x})$ represents state B, and the potential function is continuous in both λ and \mathbf{x} . The net free energy between endpoint states A and B can then be determined from the sum of free energies between a series of nonphysical but more closely spaced λ state intermediates:

$$\Delta G_{\text{tot}} = \sum_{i=1}^{\text{NWINDOW}} \Delta G_{\lambda(i-1) \rightarrow \lambda(i)} \quad (2)$$

where

$$G_{\lambda(i-1) \rightarrow \lambda(i)} = -RT \ln \langle e^{-[V(\lambda(i), \mathbf{x}) - V(\lambda(i-1), \mathbf{x})]/RT} \rangle_{\lambda(i-1)} \quad (3)$$

and NWINDOW is the number of $\delta\lambda$ intervals used. The second free energy method, thermodynamic integration (TI), is based on the fundamental equation:

$$\Delta G = \int_0^1 \left\langle \frac{dV(\lambda, \mathbf{x})}{d\lambda} \right\rangle_{\lambda} d\lambda \quad (4)$$

The integrand is evaluated at a discrete series of λ points between [0,1], and a numerical integration method is used to estimate the integral from these points.

FEP and TI both use λ intermediate states. But note that they are used for different reasons in the two approaches. In FEP, the intermediate states are *useful* to circumvent sampling difficulties. In principle, with infinite sampling or in fortuitous cases, the free energy could be precisely determined without resorting to λ intermediates. In TI, the intermediate states are *required* because the integral cannot be accurately evaluated any other way, except in the specific case where the free energy versus λ curve is approximately linear (which it usually is not). In practice, significant sampling over a series of λ states is generally required to perform quantitatively reliable free energy calculations using either method.

Until now, most efforts to improve free energy methodologies have focused on improving the quantitative predictiveness of these calculations. However, in truth, not all interesting questions require a quantitative result. In particular, one frequently wishes to determine not the effects of a specific change but rather what changes should be made to effect a desired result. To answer such questions it may be sufficient to predict the relative qualitative free energies associated with various changes. With this alternate perspective, it is worth reevaluating the possibility of performing free energy calculations from a calculation at a single λ point.

Essentially, we wish to determine if it is possible to qualitatively estimate numerous free energies from a single simulation (one window) using the FEP method.

The idea of using a single-window approach to approximate free energies for drug design is not new; early FEP work¹⁸ demonstrated this approach could be applied to estimating the contribution of a hydrogen bond to the relative free energy of binding and suggested it could be used to probe various isosteric changes. More recently, this idea has been generalized in the PROFEC¹⁹ method, so that instead of simply calculating the approximate free energy for a specific change, the same approach is used to calculate the approximate free energy at each of many grid points surrounding a molecular region of interest. A single-window free energy calculation is performed at each grid point, taking the initial reference state (state "A" in eq 1 and 2) to be the molecule itself and taking the final reference state (state "B") to be the system with a probe group at that grid point. Specifically,

$$\Delta G_{\text{gridpoint}} = -RT \ln \langle e^{-V_{\text{probe}}/RT} \rangle_{\text{no-probe}} \quad (5)$$

This is eq 1 with "no-probe" substituted for state A, "probe" substituted for state B, and replacement of $V_{\text{no-probe}}$ by 0. The probe group at every grid point consists of a single atom with nonbonded parameters representative of a united atom methyl. The free energy calculated at each grid point will suffer the same convergence problems as any single-window free energy simulation. However, by combining these grid points into a contour grid, one may be able to discern—*qualitatively*—which are the relatively more favorable regions for molecular change. Given the thousands of points that make up a standard grid with modest spacing (say, 0.5 Å), any gross inaccuracies in the individual grid points will hopefully average out sufficiently to give a qualitatively predictive grid. Preliminary results from applying this approach to a benzamide/trypsin complex appear promising.¹⁹

Here, we make two modifications to the PROFEC approach to significantly improve the applicability and usefulness of this method. First, we incorporate a "floating independent reference frame" (FIRF) for every grid point. That is, each grid point undergoes translation and rotation along with the atom of the ligand that is closest to it. In this way, the reference frame for two adjacent grid points can be different, and an appropriate free energy grid can be produced even when parts of the ligand are very flexible. Since in practice any change to the ligand will involve a covalent bond to the group being added, it makes sense that the reference frame most relevant for each grid point is defined by the closest atom of the ligand. The FIRF is automatically generated when the run is started. For flexible solutes, the FIRF is absolutely *critical* in generating a reasonable and useful grid. Thus, its introduction in OWFEG extends the applicability of the free energy grid approach to all molecules. This is a substantial improvement over PROFEC, which due to its fixed grid approach is only properly applicable to rigid molecules.

A second change in OWFEG is in the way we probe the desirability of introducing charged groups along the grid. In PROFEC, a free energy grid is generated using a neutral probe particle and eq 5. The question of whether a charged group would be better situated in that position than a neutral one is then addressed using

a free energy derivative¹⁶ with respect to charge (q) at that point calculated as:

$$dG/dq = \langle dV/dq \rangle \quad (6)$$

However, the derivative, even in the best case, is only valid in the infinitesimal regime around 0. For this reason, in the OWFEG approach we instead probe the desirability of charged groups by generating three free energy grids using eq 5. One corresponds to neutral probe groups, while the other two correspond to positively and negatively charge probe groups. The charge used for these groups is selected to be modest and representative of real charged groups. From the three grids, one can determine not only where the ligand should be modified but also whether a positive, negative, or neutral group should be used. In addition, this method will identify cases where there is more than one charge state for the added group that would bring about a desired change in the free energy profile. A free energy derivative, in contrast, can only suggest a single charge state.

To test the method, OWFEG calculations have been performed for two model systems and one protein–ligand complex. The two model systems—quinoline and “bis-pyrimidine” (4-pyrimid-2-ylmethyl-pyrimidine)—have been chosen to test the usefulness of OWFEG with both rigid and flexible molecules. The suggestions contained in the resulting free energy difference grid maps are compared to the free energies for implementing these suggestions, as calculated by standard precise TI simulations. Comparisons for these model compounds are performed at each unique hydrogen atom of both molecules. OWFEG has also been applied to the FKBP-12·FK506 protein–ligand complex. FKBP-12 is a 107-residue protein that binds the flexible 126-atom macrocycle FK506.²⁰ In this case, precise free energy calculations have been performed to test two modifications of the FK506 ligand that OWFEG suggests will improve binding. The comparisons demonstrate clearly that OWFEG is useful and predictive.

Methods

The OWFEG method has been implemented in a copy of the Amber/Sander 5.0 program.²¹ During molecular dynamics, the statistics required for three free energy grids are calculated. These grids correspond to probe groups with neutral, +0.3 e, and −0.3 e charges, respectively, in eq 5. These net charges are chosen to roughly represent the net charges on typical amino and hydroxyl groups, respectively.²² The grid is calculated around the specified molecule. Grid points are generated at equally spaced intervals for points no closer than RMIN and no further than RMAX Angstroms from the atom closest to the grid point, where RMIN and RMAX are specified by the user (see below). A floating independent reference frame (FIRF) is used. For each grid point, GP, this frame is defined by the three atoms of the molecule: the atom of the molecule that is closest to the grid point, A1; an atom connected to A1, A2; and an atom connected to A2 (other than A1), A3. Whenever possible, A2 and A3 are non-hydrogen atoms; A1 can be a hydrogen. The distance GP–A1, angle GP–A1–A2, and torsion GP–A1–A2–A3 define the reference frame. The FIRF ensures that appropriate sampling will be performed when generating a grid for a flexible molecule. The FIRF is automatically generated by the program.

For all OWFEG runs, the radius and nonbonded well depth used for the probe particle at each grid point were 2.0 Å and 0.150 kcal/mol, respectively. These values are representative

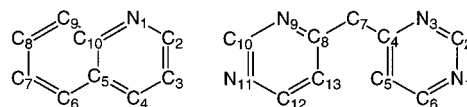


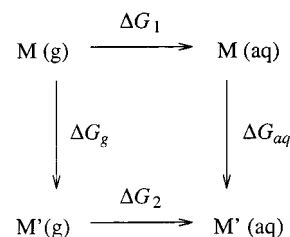
Figure 1. Schematic views of the quinoline and bis-pyrimidine molecules used to test the OWFEG method. In subsequent figures, carbon atoms of these molecules are shown in green, nitrogens are shown in blue, and hydrogens are shown in white.

of a united atom methyl group.²² Grid points were placed around the molecule such that no grid point was closer than 1.40 Å (RMIN) nor further than 2.25 Å (RMAX) from the molecule. Hydrogen atoms of the molecule were ignored in choosing the locations of the grid points. A standard grid spacing of 0.5 Å was used in each direction (x, y, z). The nonbonded potential energy V_{probe} in eq 5 is evaluated using the nonbonded pairlist of the atom of the molecule which is closest to the grid point. Only nonbonded (van der Waals and pairwise electrostatic) interactions contribute to V_{probe} :

$$V_{\text{probe}} = \sum_{i \neq j} \left\{ \left[\frac{A_{ij}}{R_{ij}^{12}} - \frac{B_{ij}}{R_{ij}^6} \right] + q_i q_j / \epsilon R_{ij} \right\} \quad (7)$$

where A_{ij} and B_{ij} are Leonard–Jones coefficients, R_{ij} is the interatomic distance between grid point i and atom j , q_i and q_j are the charges on the probe group and atom j , respectively, and ϵ is the effective dielectric constant.

All model system simulations were performed using a version of the Weiner et al. force field,²² extended to include the parameters necessary for the quinoline and bis-pyrimidine test molecules (Figure 1). Charges for these test molecules were assigned using the charge template approach in the Quanta program.²³ Each test molecule was solvated by placing it in a periodic 216 TIP3P water box²⁴ and then eliminating waters that overlapped with the solute. The system was minimized to a gradient of 0.1 kcal/mol-Å, then equilibrated using molecular dynamics (MD) for 100 ps. MD was then continued for 2 ns to perform the sampling required to evaluate the ensemble average in eq 5. All MD was carried out at constant temperature, with a dielectric constant $\epsilon = 1$. Simulations in explicit solvent were run in a periodic box at a constant pressure of 1 atm. A pairlist cutoff of 8.0 was used, and the pairlist was updated every 20 steps. The SHAKE algorithm²⁵ was applied to all bonds, and a time step of 2 fs was used. An analogous OWFEG run, but using the identical molecule in vacuo, was also performed for each test system. These vacuum simulations were required to complete the thermodynamic cycle:



M is the molecule of interest; M' is a modification of the molecular system corresponding to the molecule plus the probe group at a particular grid point; (g) and (aq) refer to the molecule in vacuum (gas) and solvated. From this free energy cycle, the experimentally relevant difference in the free energies of solvation of molecules M and M' , $\Delta G_2 - \Delta G_1$, is related to the readily calculated free energy values ΔG_{aq} and ΔG_g by the relationship:

$$\Delta G = G_2 - G_1 = \Delta G_{\text{aq}} - \Delta G_g \quad (8)$$

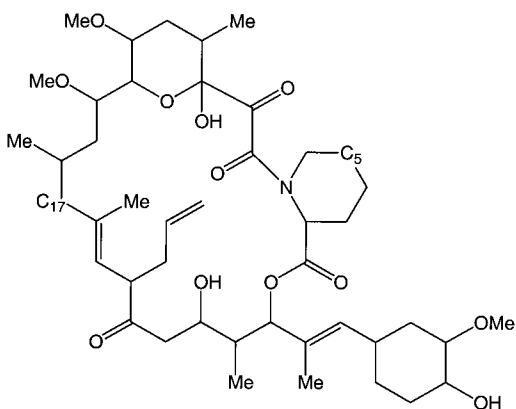


Figure 2. Schematic view of the FK506 molecule used to test the OWFEG method. In subsequent figures, carbon atoms of this molecule are shown in green, nitrogens are shown in blue, oxygens are shown in red, and hydrogens are shown in white.

The free energy differences ΔG_{aq} and ΔG_{g} were determined at each grid point; then the difference was calculated and converted to a format that could be used by the visualization program Quanta.²³ Constant energy contours are generated around the test molecule by Quanta, and from these one can infer, visually, where additional atoms can be added to the test molecule scaffold and whether these should be charged or neutral. Note that although the grid is displayed around the starting conformation of the test molecule, the FIRF approach ensures the grid energies are properly calculated to account for conformational flexibility of the molecule.

To test the predictions of the OWFEG runs, standard TI free energy calculations⁴ were performed for both test mol-

ecules. In these TI calculations, each of the unique hydrogens on the molecule was changed to (A) a united atom methyl group with no net charge change, (B) a united atom methyl group with a +0.3 e charge, (C) a united atom methyl group with a -0.3 e charge. No change in other charges in the system was made. Each free energy calculation was performed using 21 integration points with 10 ps of equilibration and 10 ps of data collection at each point. Statistical error estimates^{16,26,27} were performed during each run, to ensure that the total estimated statistical error in each simulation was <0.1 kcal/mol. Each simulation was run both forwards ($\lambda=0 \rightarrow 1$) and backwards ($\lambda=1 \rightarrow 0$), and the results were averaged. The free energy calculations were performed both for the solvated test molecules and for the test molecules in vacuo, so that, as with the OWFEG simulations, the thermodynamic cycle above would be complete. Since the nonbonded parameters used in the OWFEG simulations and in the free energy calculations are identical, the predictions from the two methods will be consistent and parameter dependence is not an issue.

OWFEG grids have been generated and free energy simulations performed, for two test molecules: quinoline and bis-pyrimidine. A total of 7 678 grid points surround the quinoline and 10 209 grid points surround the bis-pyrimidine.

As an additional test of the method, OWFEG calculations have also been performed for the FKBP-12-FK506 protein-ligand complex. FK506 is a 126-atom macrocycle with considerable intrinsic flexibility and FKBP-12 is a 107-residue protein.²⁰ The FK506 ligand in these simulations was parameterized as described previously,²⁸ while the FKBP-12 protein was parameterized using the standard Weiner et al. force field; 11 counterions were added to the complex to achieve net neutrality. The FKBP-12-FK506 complex was then placed in a periodic water box of 3836 waters, with dimensions of approximately $59 \times 48 \times 46$ Å. This system was minimized

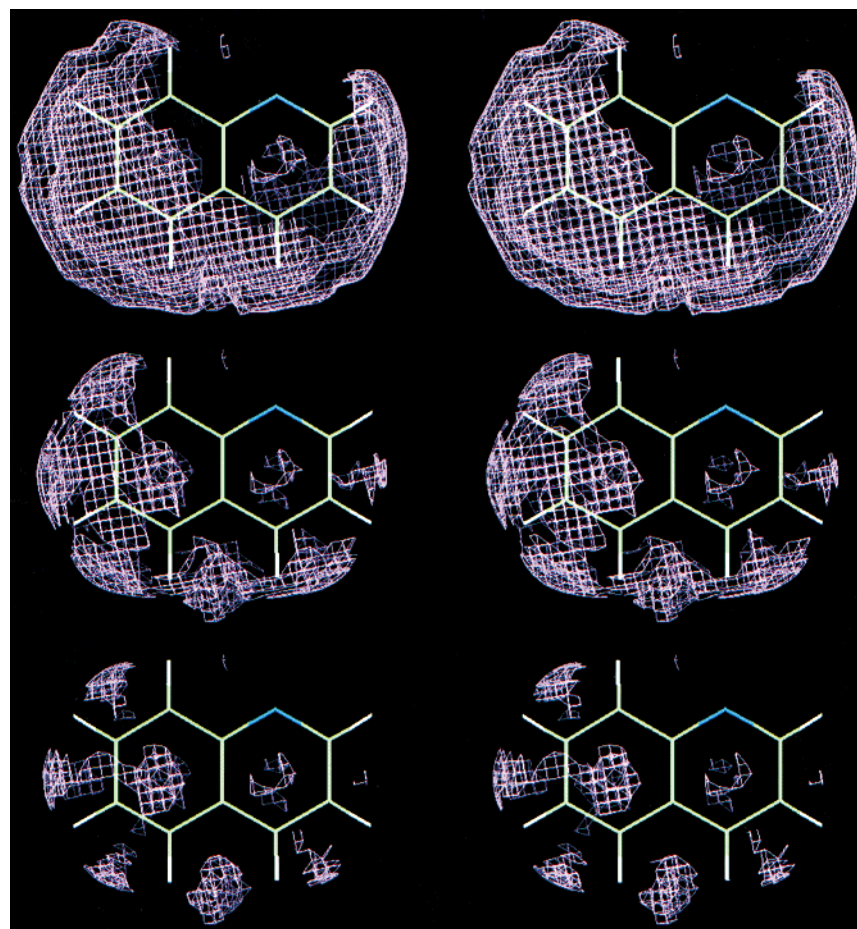


Figure 3. OWFEG difference map ($\Delta G_{\text{aq}} - \Delta G_{\text{g}}$) for quinoline, corresponding to a neutral probe group. The top, middle, and bottom figures correspond to contours at 1.0, 0.25, and 0.0 kcal/mol, respectively. The figures are shown in stereo.

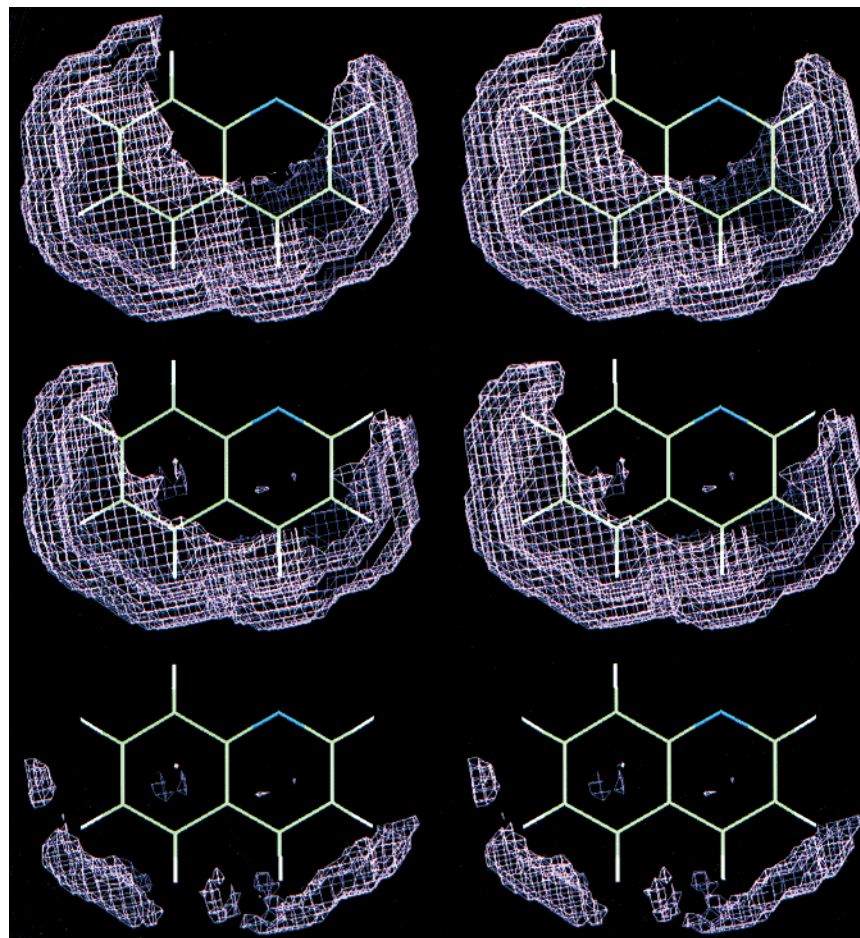
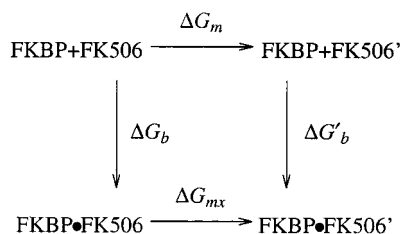


Figure 4. OWFEG difference map ($\Delta G_{\text{aq}} - \Delta G_{\text{b}}$) for quinoline, corresponding to a positive (+0.3 e) probe group. The top, middle, and bottom figures correspond to contours at 0.0, -5.0, and -10.0 kcal/mol, respectively. The figures are shown in stereo.

and then equilibrated for 80 ps at 300 K, at a constant pressure of 1 atm, and using a time step of 2 fs. MD was carried out at constant temperature, with a dielectric constant $\epsilon = 1$, and at a constant pressure of 1 atm. An 8 Å cutoff was used, and the pairlist was updated every 20 steps. To complete the thermodynamic cycle, a second system consisting of FK506 in water was constructed; 992 waters were used to solvate the FK506 molecule, giving a box of approximately $34 \times 34 \times 27$ Å. Simulations of this FK506 system were performed analogously to those of the FKBP-12·FK506 complex.

OWFEG grids were generated for both the FKBP-12·FK506 and FK506 systems, using the same parameters and procedures as described for the model systems above. These two OWFEG grids were used to probe the thermodynamic cycle:



FK506 is the standard FK506 macrocycle, and FK506' represents FK506 modified by introducing a new group. At each point of the OWFEG grid, we represent $\Delta G_{\text{mx}} - \Delta G_m$ for introducing the probe group at that point. This is directly related to the experimental differential free energy for introducing that group at that point by

$$\Delta \Delta G = \Delta G_{\text{mx}} - \Delta G_m = G'_b - G_b \quad (9)$$

where G'_b and G_b are experimental measurable. A total of 5 251 grid points were generated for the FK506 OWFEG runs.

The OWFEG grids for FKBP-12·FK506 were examined to locate changes which were predicted to have large favorable effects on the relative binding of the modified FK506 to the protein. Two changes which appeared from these grids to offer among the largest improvement in binding free energy (reduction in $\Delta \Delta G$) were tested by performing precise TI free energy calculations. The two suggested changes correspond to introduction of a positively charged probe group (+0.3 e) off C33 and to introduction of a negatively charged probe group (-0.3 e) off C17 (Figure 2). The charges of the hydrogen atoms off C33 (H36) and C17 (H19) in the FK506 model are 0.1757 and 0.1207 e, respectively. The TI simulations were performed using 21 integration points; 10 ps of equilibration and 10 ps of data collection were performed at every point. Statistically-based error analysis was performed at each integration point to ensure that the total statically-based error in each simulation was <0.2 kcal/mol. The free energies were calculated both forwards ($\lambda=0 \rightarrow 1$) and backwards ($\lambda=1 \rightarrow 0$), and the results were averaged. A total of four pairs of simulations were carried out: These correspond to ΔG_{mx} and ΔG_m , both forwards and backwards, for both the C33 and C17 changes. From these, the net $\Delta \Delta G$ values for both changes were determined.

Unlike the model system calculations, where the TI calculations were performed to confirm the qualitative rankings of the OWFEG grids, in this case we were more concerned with demonstrating that the OWFEG grids could be used in a *practical* sense to suggest changes to a molecule. This means we need to be concerned with maintaining the net neutrality of the system. For example, if a hydroxyl group is introduced at a location where a negatively charged probe group is suggested, the net charge on the *system* will not change. Neutrality was maintained in a very simple manner, by

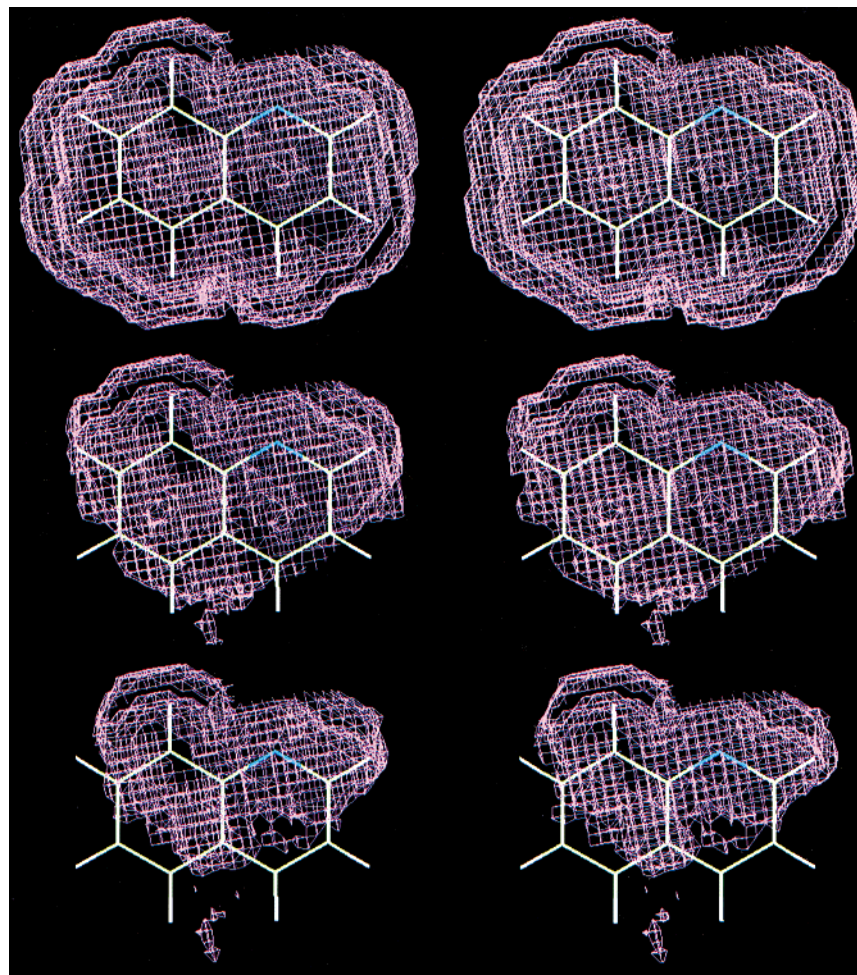


Figure 5. OWFEG difference map ($\Delta G_{\text{aq}} - \Delta G_{\text{g}}$) for quinoline, corresponding to a negative ($-0.3 e$) probe group. The top, middle, and bottom figures correspond to contours at 0.0, -5.0 , and -7.5 kcal/mol, respectively. The figures are shown in stereo.

assuming that the effects of changing the charge on a substituent would be relatively local. Thus, the negative of the change in charge in going from a hydrogen to the charge on the probe group was distributed in equal part among the carbon attached to the hydrogen that was being changed and to all first and second heavy atom neighbors of this carbon. The nonbonded parameters of the hydrogen were changed to those of the probe group used in generating the OWFEG map, and the bond and angle parameters to the probe group were changed to mimic those to a standard aliphatic carbon. (Use of other bond/angle parameters, such as those corresponding to nitrogen or carbon, yielded results that are very similar.)

Results

As a first test of the OWFEG method, it was applied to a quinoline molecule (Figure 1). Quinoline was chosen for its rigidity and because the atomic asymmetry resulting from the ring nitrogen results in seven unique locations where substitution of a hydrogen by the probe group could occur. Three contours of the resulting OWFEG difference ($\Delta G_{\text{aq}} - \Delta G_{\text{g}}$) maps are shown in Figures 3–5. Figure 3 presents contours corresponding to introduction of a neutral probe group. Figures 4 and 5 present contours corresponding to positively and negatively charged probe groups, respectively. From these figures, one can rank the unique hydrogen positions in the molecule in terms of how favorable (or unfavorable) it would be to introduce a probe group at or near that position. The qualitative rankings derived from the grids are given in Table 1.

To test the OWFEG predictions, free energy simulations were performed at each unique hydrogen position. The hydrogen was “mutated” into a probe group with the same nonbonded parameters as the probe group in the OWFEG simulation. Three free energy calculations were performed at each location, corresponding to changing the hydrogen into the probe group with no net charge change, into a positively charged probe group with the probe group charge, and into a negatively charged probe group with the probe group charge. Each free energy simulation was performed twice, once in solvent and once in vacuum, to yield the required $\Delta\Delta G$ difference (eq 7). To ensure the free energy values being calculated would be most directly comparable to the values being predicted in the OWFEG calculations, only the charge of the hydrogen being changed was modified during the calculation. The remaining charges in the system were held fixed.

The free energy values calculated in this fashion are presented in Table 1. The free energies are rank-ordered, best (1) to worst (7). To aid in comparisons with the qualitative rankings from OWFEG, free energies closer than 0.5 kcal/mol were considered to be the same in terms of rank order. Comparing the rank order of the exact TI values with those from OWFEG, it is seen that the OWFEG maps allow excellent qualitative predictions. In the case of the neutral probe, the qualitative rankings of all seven positions, based on TI,

Table 1. Free Energy Rankings for Quinoline Hydrogen Positions

| hydrogen position | probe charge ^b | TI simulation ^a | | OWFEG ranking ^c |
|-------------------|---------------------------|----------------------------|----------------------|----------------------------|
| | | ΔG_{calc} | ranking ^c | |
| C2 | 0.00 | +0.15 | 1 | 5 |
| C3 | 0.00 | +0.47 | 1 | 5 |
| C4 | 0.00 | +0.10 | 1 | 1 |
| C6 | 0.00 | +0.13 | 1 | 1 |
| C7 | 0.00 | +0.16 | 1 | 1 |
| C8 | 0.00 | +0.14 | 1 | 1 |
| C9 | 0.00 | +0.21 | 1 | 5 |
| C2 | +0.30 | -0.25 | 6 | 6 |
| C3 | +0.30 | -2.50 | 1 | 1 |
| C4 | +0.30 | -2.79 | 1 | 1 |
| C6 | +0.30 | -2.96 | 1 | 1 |
| C7 | +0.30 | -2.98 | 1 | 1 |
| C8 | +0.30 | -1.46 | 5 | 5 |
| C9 | +0.30 | +2.11 | 7 | 7 |
| C2 | -0.30 | -16.72 | 2 | 2 |
| C3 | -0.30 | -6.80 | 7 | 4 |
| C4 | -0.30 | -7.75 | 4 | 4 |
| C6 | -0.30 | -7.98 | 4 | 4 |
| C7 | -0.30 | -7.94 | 4 | 4 |
| C8 | -0.30 | -11.93 | 3 | 3 |
| C9 | -0.30 | -24.52 | 1 | 1 |

^a ΔG is $\Delta G_{\text{aq}} - \Delta G_{\text{g}}$ as in eq 8. Numerical free energies were determined using the thermodynamic integration technique. Values are given in kcal/mol. Values represent the average of "forward" ($\lambda=0 \rightarrow 1$) and "backward" ($\lambda=1 \rightarrow 0$) simulations. The error in each value, estimated by statistical means, is <0.10 kcal/mol. ^b The charge of each hydrogen in the quinoline molecule is 0.165 e. All charges in e. ^c Relative ranking of the position in terms of how favorable it would be to change the hydrogen at that position to a probe group. A ranking of 1 is most favorable and 7 is least favorable. OWFEG rankings are qualitatively determined from contour plots about the molecule like those in Figures 2–4. For positions with very similar contour grids, an identical ranking is given. For rankings based on TI results, positions with ΔG 's differing by <0.5 kcal/mol are assigned equal rankings. Equally ranked positions are all assigned the same number.

are the same, and the ΔG for the change at each position is positive. This is consistent with the OWFEG rankings, although the OWFEG calculations indicate a modest preference for the C4, C6, C7, and C8 positions. By reference to Figure 3, it can be seen that none of the hydrogen positions fall within the ≤ 0 kcal/mol energy contours. For the positively charged probe, the rankings from TI and OWFEG are identical. For the negatively charged probe, the TI and OWFEG rankings are also identical, with the exception of the C3 position. This position is less favorable than positions C4, C6, and C7 by TI but cannot be distinguished from those positions by OWFEG.

Having shown OWFEG capable of useful predictions in the case of a rigid solute (where the choice of reference frame for the grid points is straightforward), we applied the method to a molecule that undergoes conformational changes. The bis-pyrimidine molecule (Figure 1) was chosen for its intrinsic simplicity and for its symmetry. The symmetry provides a check on whether the results obtained using OWFEG are reasonably converged, since the grids for both symmetric halves of the molecule should be the same.

As can be seen in Figure 6, the two aromatic rings in the bis-pyrimidine undergo continual moderate fluctuations within a broad local minimum. Less frequently, they also undergo large conformational transitions. The transitions for the two rings are not closely correlated. As a result of these fluctuations, it is not possible to

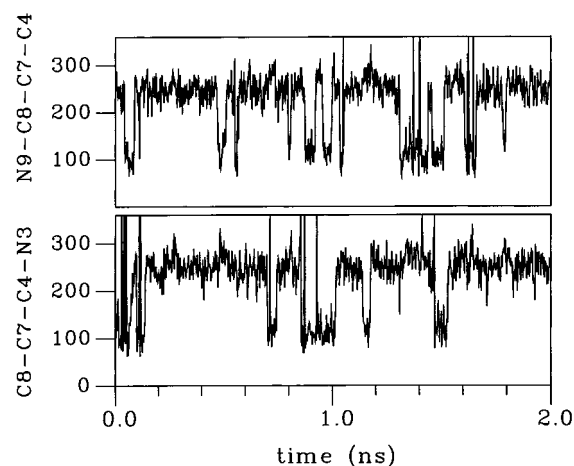


Figure 6. Fluctuations of the dihedral angles that connect the two rings in bis-pyrimidine to the central methylene. Note that these two rings undergo considerable fluctuation and that the fluctuations are not tightly correlated. For this reason, a single reference frame appropriate for all surrounding grid points cannot be defined.

define a single reference frame that makes sense for all the grid points surrounding the molecule. The FIRF circumvents this problem. Using the FIRF, each grid point is defined relative to the reference frame of the closest atom of the molecule.

Three contours of the resulting OWFEG difference grids are presented in Figures 7–9. These figures correspond to neutral, positively charged, and negatively charged probe groups, respectively. Note that the contours are reasonably symmetric, as they should be if the grid points are sufficiently converged to be qualitatively predictive. From the contours, the four unique hydrogen positions have been ranked in terms of how favorable or unfavorable a change to the probe group at the position would be. The rankings are presented in Table 2.

For comparison, standard TI free energy simulations were also performed at each of the four unique hydrogen positions, in the same fashion as for quinoline (above). The results and rankings from these standard TI calculations are also presented in Table 2. It can again be seen that the OWFEG relative rankings are in good qualitative agreement with the results from the TI simulations. The only differences occur where two positions that are similar but distinguishable by TI are qualitatively indistinguishable from OWFEG.

As has been noted, the success of OWFEG for flexible molecules is due to the use of FIRF. To demonstrate this, a second set of OWFEG simulations was performed for the bis-pyrimidine molecule where only a single reference frame was used. The reference frame was defined by the carbon of the methylene group that joins the two pyrimidines (C7) and two carbons of one attached ring (C4, C5). The resulting OWFEG difference map is presented in Figure 10. As can be clearly seen, using a single reference frame one does not produce the expected grid symmetry. From this OWFEG grid, it would appear that the three hydrogen positions on the left-hand pyrimidine in the figure are significantly different from the three on the right with respect to changes to the probe atoms. This, of course, makes no physical sense.

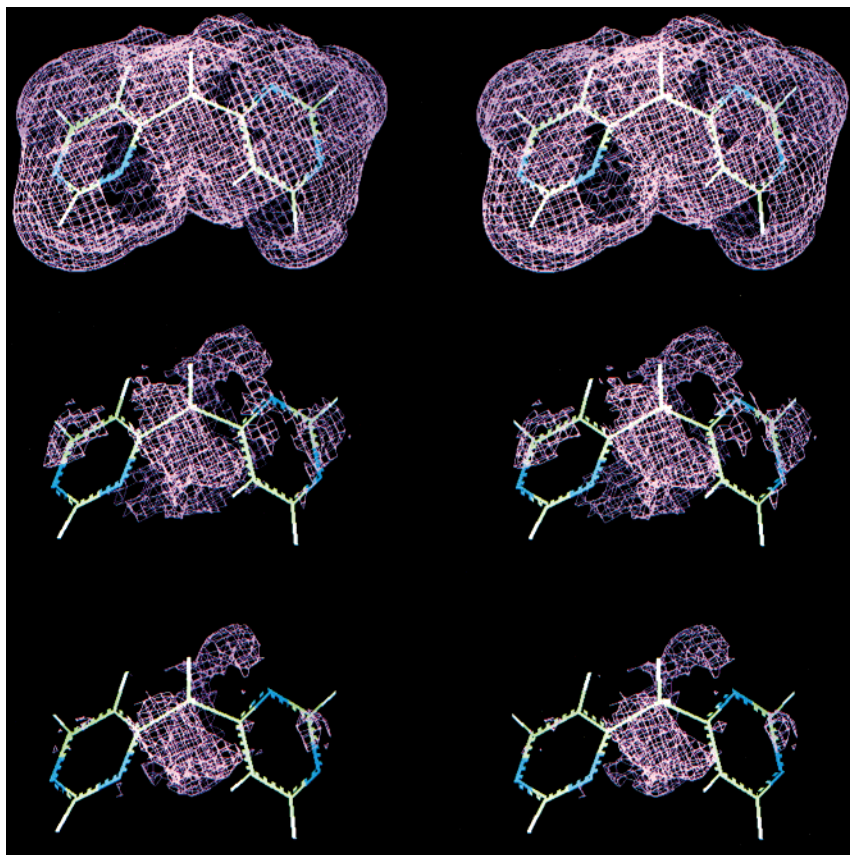


Figure 7. OWFEG difference map ($\Delta G_{\text{aq}} - \Delta G_{\text{g}}$) for bis-pyrimidine, corresponding to a neutral probe group. The top, middle, and bottom figures correspond to contours at 1.0, 0.0, and -1.0 kcal/mol, respectively. The figures are shown in stereo.

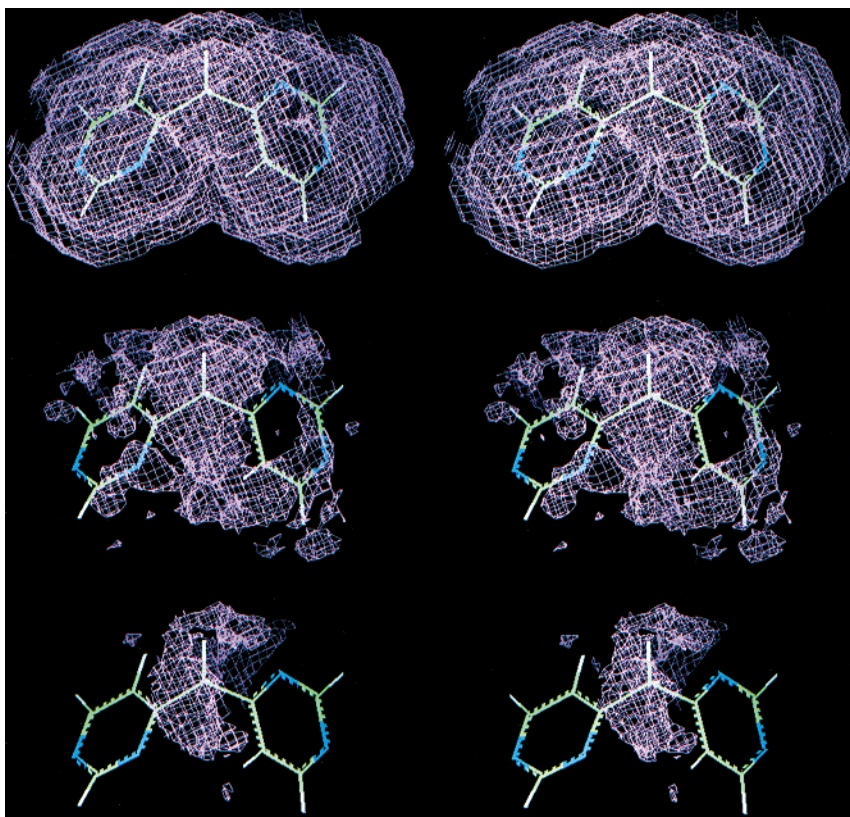


Figure 8. OWFEG difference map ($\Delta G_{\text{aq}} - \Delta G_{\text{g}}$) for bis-pyrimidine, corresponding to a positive ($+0.3$ e) probe group. The top, middle, and bottom figures correspond to contours at 0.0, -8.0 , and -10.0 kcal/mol, respectively. The figures are shown in stereo.

Having satisfied ourselves that the method could perform well on model systems, OWFEG was applied

to the FKBP-12·FK506 protein–ligand complex as a final test. The OWFEG grid corresponding to $\Delta G_{\text{mx}} -$

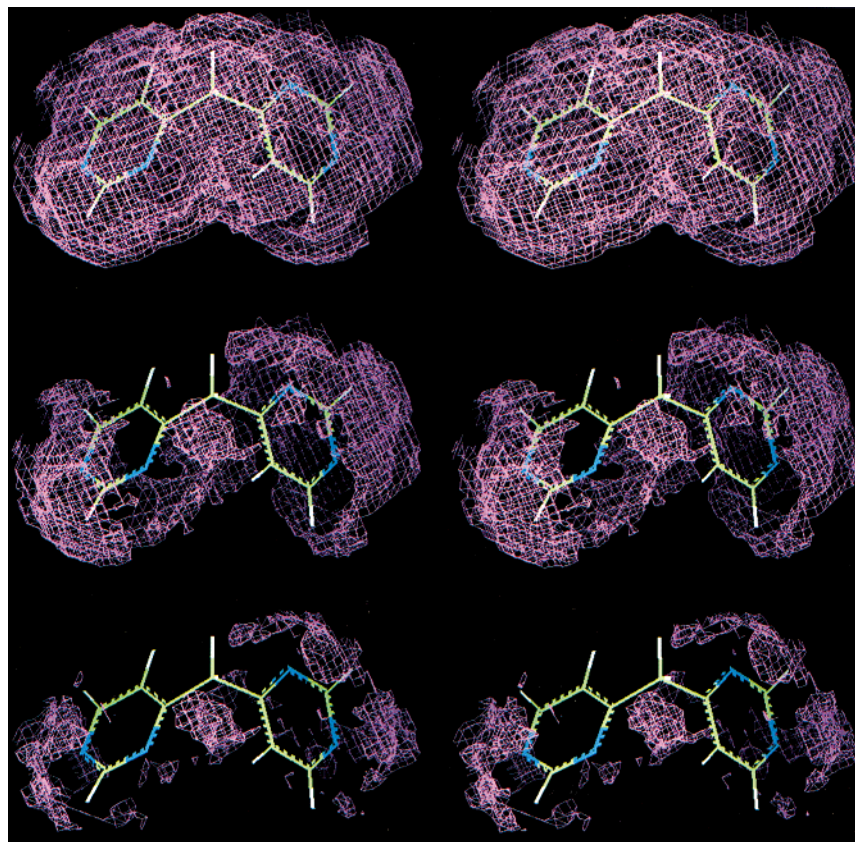


Figure 9. OWFEG difference map ($\Delta G_{\text{aq}} - \Delta G_{\text{g}}$) for bis-pyrimidine, corresponding to a negative (-0.3 e) probe group. The top, middle, and bottom figures correspond to contours at 0.0, -5.0 , and -7.0 kcal/mol, respectively. The figures are shown in stereo.

Table 2. Free Energy Rankings for Bis-pyrimidine Hydrogen Positions

| hydrogen position | probe charge ^b | TI simulation ^a | | OWFEG ranking ^b |
|-------------------|---------------------------|----------------------------|----------------------|----------------------------|
| | | ΔG_{calc} | ranking ^b | |
| C5 | 0.00 | +0.96 | 1 | 1 |
| C6 | 0.00 | +0.58 | 1 | 1 |
| C2 | 0.00 | +0.80 | 1 | 1 |
| C7 | 0.00 | +0.88 | 1 | 1 |
| C5 | +0.30 | -4.06 | 2 | 2 |
| C6 | +0.30 | -2.79 | 3 | 3 |
| C2 | +0.30 | -1.97 | 4 | 3 |
| C7 | +0.30 | -6.73 | 1 | 1 |
| C5 | -0.30 | -2.04 | 3 | 2 |
| C6 | -0.30 | -9.12 | 2 | 1 |
| C2 | -0.30 | -10.87 | 1 | 1 |
| C7 | -0.30 | -1.61 | 3 | 2 |

^a ΔG is $\Delta G_{\text{aq}} - \Delta G_{\text{g}}$ as in eq 8. Numerical free energies were determined using the thermodynamic integration technique. Values are given in kcal/mol. Values represent the average of "forward" ($\lambda=0 \rightarrow 1$) and "backward" ($\lambda=1 \rightarrow 0$) simulations. The error in each value, estimated by statistical means, is <0.10 kcal/mol.

^b The charge of each ring hydrogen in the bis-pyrimidine molecule is 0.104 e. The charge of the hydrogens in the methylene group (C7) is 0.024 e. All charges in e. ^c Relative ranking of the position in terms of how favorable it would be to change the hydrogen at that position to a probe group. A ranking of 1 is most favorable and 4 is least favorable. OWFEG rankings are qualitatively determined from contour plots about the molecule like those in Figures 6–8. For positions with very similar contour grids, an identical ranking is given. For rankings based on TI results, positions with ΔG 's differing by <0.5 kcal/mol are assigned equal rankings. Equally ranked positions are all assigned the same number.

ΔG_{m} in eq 9 was generated for the neutral, positively, and negatively charged probe groups. From these, the most obvious suggestions of changes that could decrease the net $\Delta\Delta G$ came from the maps for the positively and

negatively charged probe group. Representatives of these maps are shown in Figure 11. The maps were plotted at successively lower (more negative) contour values until only a select few lowest-energy sites remained. From these, sites were selected on the basis of two criteria: (1) they appeared to present the largest regions of negative free energy located close to replaceable hydrogens on the molecule; (2) they differentiated the different maps, i.e. peaks that were comparably large at low contours in two or more maps were ignored.

From these criteria, two sites, in particular, stand out from these maps. In the map corresponding to a positively charged probe (Figure 11, top), the site chosen is a hydrogen (H36) off atom C33. In the map corresponding to a negatively charged probe (Figure 11, bottom), the site chosen is a hydrogen (H19) off atom C17 (see Figure 2 for the atom name legend). No site in the neutral probe free energy map was as suggestive as these, and so we concentrated on the aforementioned two sites only. The precise $\Delta\Delta G$ free energy differences for changing H36 to a positively charged probe atom and H19 to a negatively charged probe atom were calculated using TI, as described in the Methods section. As noted, the net charge on the system was not changed in these TI simulations; the negative of the change in charge in going from the hydrogen to the probe group was evenly distributed on the attached carbon and all first and second neighbor heavy atoms. The resulting $\Delta G_{\text{mx}} - \Delta G_{\text{m}}$ free energy differences were calculated to be -1.1 ± 0.2 and -0.55 ± 0.3 kcal/mol, respectively, for the H36 and H19 perturbations. Both values are negative (improved binding), as predicted by the OWFEG grid. Note that the magnitudes of these $\Delta\Delta G$ values are

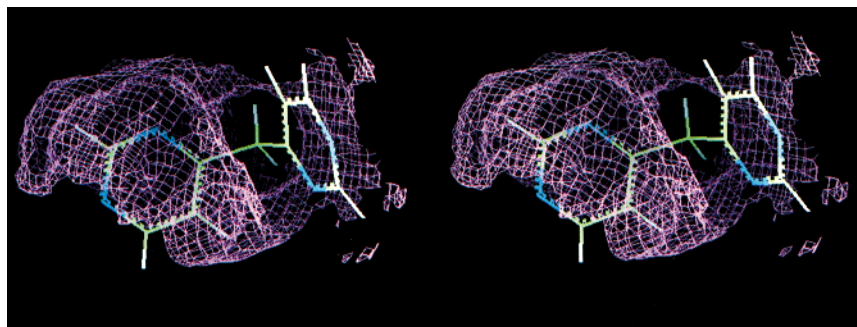


Figure 10. OWFEG difference map ($\Delta G_{\text{aq}} - \Delta G_{\text{g}}$) for bis-pyrimidine, corresponding to a neutral probe group. This map was generated using a single reference frame for all grid points. The reference frame was defined by the methylene carbon and two carbons of the ring to the right in the figure. The map is contoured at 0.0 kcal/mol. The figure is shown in stereo.

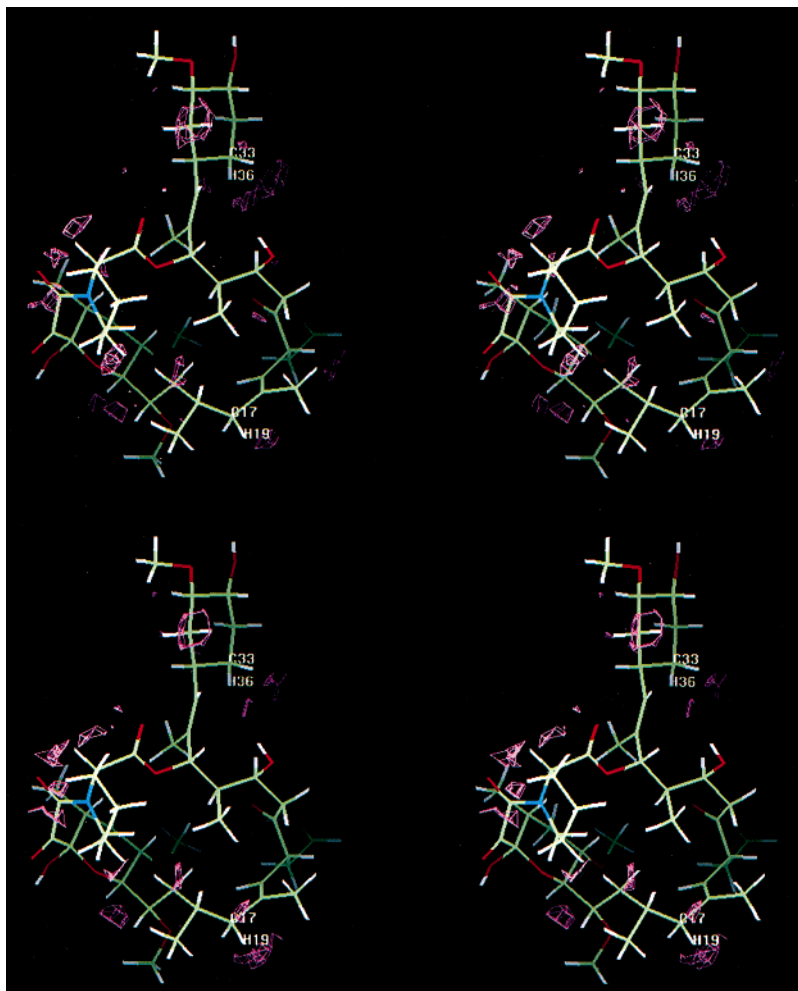


Figure 11. OWFEG difference map ($\Delta G_{\text{mx}} - \Delta G_{\text{m}}$; eq 9) for the FKBP-12·FK506 complex. The top map corresponds to a positive (+0.3 e) probe group, contoured at -20 kcal/mol. The bottom map corresponds to a negative (-0.3 e) probe group, contoured at -35 kcal/mol. Both contour levels were chosen to isolate those regions resulting in the largest negative changes in $\Delta\Delta G$. The hydrogen atoms chosen for precise TI calculations and their attached carbon atoms are labeled. The 2-D representation is given in Figure 2. The figures are shown in stereo.

modest, as one would expect, and nowhere near the values in the free energy grids that were used to predict them. This is because the free energy grids correspond to effectively introducing a net charge into the system (the charges on the remainder of the system are not modified). The fact that the qualitative predictions of the maps hold when net neutrality of the system is maintained attests to the true usefulness of the OWFEG grids.

Discussion

It has been demonstrated that the OWFEG method can generate a qualitative predictive free energy grid about a molecule. This has been shown for two model tests systems, quinoline and bis-pyrimidine, and for a protein–ligand system, FKBP-12·FK506. The predictions derived using OWFEG have been compared with free energies calculated using precise standard thermodynamic integration simulations. The model system

results demonstrate that the qualitative results derived from the two methods are in excellent agreement, in terms of the rank order of free energies for changing the hydrogens to probe groups. And the protein–ligand results demonstrate that the OWFEG maps have *practical* use for real systems, where charge redistribution upon adding a charged group will occur.

The FIRF that OWFEG uses is a critical new feature of this grid based approach. Using the FIRF, the reference frame for each grid point is defined by the atom of the molecule closest to the grid point. Without the FIRF, the applicability of the free energy grid is limited to rigid solutes. The rigid molecule limitation is a major drawback of the antecedent PROFEC method, which uses a single reference frame for all grid points. As has been shown, for a nonrigid molecule such as the bis-pyrimidine or FK506 here, a reliable free energy grid can only be generated by assigning reference frames for grid points that depend on what part of the molecule they are proximate to. In principle, one could do the same thing manually with PROFEC and then run separate simulations to generate grids about the independently varying moieties of the molecule. But this can be cumbersome and inefficient, and one runs the risk of misassigning grid points, particularly for complex systems.

OWFEG also differs from PROFEC in how the effects of a change to the charge of a probe group are probed. OWFEG uses finite FEP-based changes, while PROFEC probes these changes using free energy derivatives. It is expected that the finite probe method used by OWFEG will be preferable in many cases, since the derivatives are only completely reliable in the infinitesimal regime about $\delta\text{charge} = 0$. For the model systems tested here, the OWFEG approach to probing charge changes appears to work well.

Several caveats should be noted with regard to this work. First and foremost is the fact that in a sense, the potential changes probed by the work presented here are of the simplest type: replacement of an existing moiety on the molecule (hydrogen) by another (the probe group). It will probably be more difficult to obtain predictive results for grid points at a significant distance from the molecule being probed. The further one moves from the molecule, the greater the difference between the reference state and the probe state (states “A” and “B” in eq 5). In addition, once one moves beyond groups that are directly attached to the molecule, other complications arise. In particular, the OWFEG method does not include any contributions from internal coordinates (bonds, valence angles, and torsion). While these will probably be modest for changes like those examined here, they could be substantial when two or more additional groups are added. For example, the entropic consequences of a growing saturated multiatom side chain can be substantial. And the fact that we are considering probe groups with a prechosen net charge might obscure the true preferences about a molecule if the free energy varies sharply with charge and undergoes a reversal in the sign of the net free energy around the value of the probe charge. Finally, in the model system tests, we have made no attempt here to account for the free energy effects of redistribution of charge that would occur when adding a group to a molecule (though

we have incorporated charge redistribution in the FKBP-12·FK506 test).

Related to this last item, it is important to keep in mind that the free energies determined by the OWFEG grids are not exactly the same as the free energies determined in the TI calculations. Specifically, for the OWFEG free energies to be the same, the reference state for each grid point would have to be the hydrogen being replaced, rather than “nothing” (no-probe) as in eq 5. However, to use the hydrogens as the reference state would be biasing the results in the desired direction. In the general case, one would use OWFEG to look for favorable locations for probe groups both near *and away from* the hydrogen atoms of the molecule. So, to more accurately reflect the manner in which OWFEG would be run, we chose to use the “no-probe” reference state. The good agreement between the OWFEG predictions and TI calculations in spite of this difference provides hope that OWFEG will be generally applicable. And the results for the FKBP·FK506 system confirm that despite these caveats with respect to charge redistribution and change in the OWFEG maps, the maps *are* predictive for real systems.

In total, the results here suggest that OWFEG may be able to side-step the above potential caveats in many cases, especially if one is careful to keep in mind the strictly *qualitative* nature of the results. An earlier report of results using the similar PROFEC approach for a benzamide/trypsin complex also supports use of free energy grid methods.¹⁹ However, the present results offer even more substantial affirmation of the method, since the predictions here were compared directly to precise free energy results using the same force-field parameters, and OWFEG has been applied to the more general case of a conformationally flexible ligand.

Overall, these results are quite exciting, as methods such as OWFEG and PROFEC appear to dramatically expand the usefulness of free energy methods as applied to drug design.

Acknowledgment. Gratitude is extended to Peter Kollman, who provided a preprint of the PROFEC results.

References

- (1) Postma, J. P. M.; Berendsen, H. J. C.; Haak, J. R. Thermodynamics of cavity formation in water. *Faraday Symp. Chem. Soc.* **1982**, *17*, 55–67.
- (2) Tembe, B. L.; McCammon, J. A. Ligand-receptor interactions. *Comput. Chem.* **1984**, *8*, 281–283.
- (3) Jorgensen, W. L.; Ravimohan, C. Monte Carlo simulation of differences in free energies of hydration. *J. Chem. Phys.* **1985**, *83*, 3050–3054.
- (4) Pearlman, D. A.; Rao, B. G. Free energy calculations: methods and applications. In *Encyclopedia of Computational Chemistry*; Schleyer, P. V. R., Allinger, N. L., Clark, T., Gasteiger, J., Kollman, P. A., Schaefer III, H. F., Schreiner, R. P., Eds.; John Wiley & Sons: New York, 1998; pp 1036–1061.
- (5) Kollman, P. Free energy calculations—applications to chemical and biochemical phenomena. *Chem. Rev.* **1993**, *93*, 2395–2417.
- (6) Pearlman, D. A.; Connelly, P. R. Determination of the differential effects of hydrogen bonding and water release on the binding of FK506 to native and Tyr82 → Phe82 FKBP-12 proteins using free energy simulations. *J. Mol. Biol.* **1995**, *248*, 696–717.
- (7) Karplus, M.; McCammon, J. A. Dynamics of proteins: elements and function. *Annu. Rev. Biochem.* **1983**, *52*, 263–300.
- (8) Jorgensen, W. L. Theoretical studies of medium effects on conformational equilibria. *J. Phys. Chem.* **1983**, *87*, 5304–5314.
- (9) Pearlman, D. A.; Kollman, P. A. The Overlooked Bond-Stretching Contribution in Free Energy Perturbation Calculations. *J. Chem. Phys.* **1991**, *94*, 4532–4545.

- (10) Straatsma, T. P.; McCammon, J. A. Multiconfiguration Thermodynamic Integration. *J. Chem. Phys.* **1991**, *95*, 1175–1188.
- (11) Mitchell, M. J.; McCammon, J. A. Free energy difference calculations by thermodynamic integration—difficulties in obtaining a precise value. *J. Comput. Chem.* **1991**, *12*, 271–275.
- (12) Mazor, M.; Pettitt, B. M. Convergence of the chemical potential in aqueous simulations. *Mol. Simul.* **1991**, *6*, 1–4.
- (13) Fleischman, S. H.; Zichi, D. A. Free energy simulations of methane solvation—a study of integrand convergence properties using thermodynamic integration. *J. Chim. Phys.* **1991**, *88*, 2617–2622.
- (14) Hodel, A.; Simonson, T.; Fox, R. O.; Brunger, A. T. Conformational Substates and Uncertainty in Macromolecular Free Energy Calculations. *J. Phys. Chem.* **1993**, *97*, 3409–3417.
- (15) Pearlman, D. A. Determining the Contributions of Constraints in Free Energy Calculations: Development, Characterization, and Recommendations. *J. Chem. Phys.* **1993**, *98*, 8946–8957.
- (16) Pearlman, D. A. Free Energy Derivatives: A New Method for Probing the Convergence Problem in Free Energy Calculations. *J. Comput. Chem.* **1994**, *15*, 105–123.
- (17) Helms, V.; Wade, R. C. Free energies of hydration from thermodynamic integration: Comparison of molecular mechanics force fields and evaluation of calculation accuracy. *J. Comput. Chem.* **1997**, *18*, 449–462.
- (18) Lau, W. F.; Pettitt, B. M. Selective Elimination of Interactions: A Method for Assessing Thermodynamic Contributions to Ligand Binding with Application to Rhinovirus Antivirals. *J. Med. Chem.* **1989**, *32*, 2542–2547.
- (19) Radmer, R. J.; Kollman, P. A. The application of three approximate free energy calculations methods to structure based ligand design: Trypsin and its complex with inhibitors. *J. Comput.-Aided Mol. Des.* **1998**, *12*, 215–227.
- (20) Schreiber, S. L. Chemistry and biology of the immunophilins and their immunosuppressive ligands. *Science* **1991**, *251*, 283–287.
- (21) Case, D. A.; Pearlman, D. A.; Caldwell, J. C.; Cheatham III, T. E.; Ross, W. S.; Simmerling, C.; Darden, T.; Merz, K. M.; Stanton, R. V.; Cheng, A.; Vincent, J. J.; Crowley, M.; Ferguson, D. M.; Radmer, R.; Seibel, G. L.; Singh, U. C.; Weiner, P.; Kollman, P. A. AMBER Pearlman 5.0; University of California: San Francisco, 1997.
- (22) Weiner, S. J.; Kollman, P. A.; Nguyen, D. T.; Case, D. A. An All Atom Force Field for Simulations of Proteins and Nucleic Acids. *J. Comput. Chem.* **1986**, *7*, 230–252.
- (23) Quanta97; Molecular Simulations Incorporated: San Diego, CA, 1997.
- (24) Jorgensen, W. L.; Chandrasekhar, J.; Madura, J.; Impey, R. W.; Klein, M. L. Comparison of simple potential functions for simulating water. *J. Chem. Phys.* **1983**, *79*, 926–935.
- (25) Ryckaert, J. P.; Ciccotti, G.; Berendsen, H. J. C. Numerical Integration of the Cartesian Equations of Motion of a System with Constraints: Molecular Dynamics of n-Alkanes. *J. Comput. Phys.* **1977**, *23*, 327–341.
- (26) Davenport, W. B. *Probability and Random Processes*; McGraw-Hill: New York, 1970.
- (27) Straatsma, T. P.; Berendsen, H. J. C.; Stam, A. J. Estimation of Statistical Errors in Molecular Simulation Calculations. *Mol. Phys.* **1986**, *57*, 89–95.
- (28) Pearlman, D. A. How is an NMR structure best defined? An analysis of molecular dynamics distance-based approaches. *J. Biomol. NMR* **1994**, *4*, 1–16.

JM990133Z